Network-Based Fuzzy Decentralized Sliding-Mode Control for Car-Like Mobile Robots

Chih-Lyang Hwang, *Associate Member, IEEE*, Li-Jui Chang, *Associate Member, IEEE*, and Yuan-Sheng Yu

***Abstract*—In this paper, the trajectory tracking of a car-like mobile robot (CLMR) using network-based fuzzy decentralized sliding-mode control (NBFDSMC) is developed. The scaling factors and the coefficients of the sliding surface for the control of the steering angle and forward–backward velocity of a CLMR are adopted by that for the control of two motors. Due to the delay transmission of a signal through an Internet and wireless module, a revision of fuzzy decentralized sliding-mode control (FDSMC) with suitable sampling time (i.e., NBFDSMC) is accomplished by the quality-of-service (QoS). The proposed control can track a reference trajectory without the requirement of a mathematical model. Only the information of the upper bound of system knowledge (including the dynamics of the CLMR, the delay feature of Internet network, and wireless module) is required to select the suitable scaling factors and coefficients of sliding surface such that an excellent performance is obtained. In addition, the stability of the closed-loop system in the presence of time-varying delay is addressed. Finally, a sequence of experiments including the control of unloaded CLMR and the trajectory tracking of CLMR is carried out to consolidate the usefulness of the proposed control system.**

***Index Terms*—Car-like mobile robot (CLMR), decentralized control, fuzzy sliding-mode control (FSMC), network-based control, proportional-integral-derivative (PID) control, wireless communication device.**

I. Introduction

AS ONE KNOWS, a time-delay (or dead time) is frequently encountered in various dynamic systems. Such time-delay systems generally arise as a result of delay in transmission of information between different parts of the system (e.g., delay caused by the low-bandwidth transmission lines, slow acoustical connections, or long satellite transmissions) [1]–[5]. Recently, Tipsuwan and Chow [6] also discuss a survey paper of networked-based control methodologies. The above-mentioned papers conclude that the feedback control (or networked-based control) in the face of time-delay always results in a limit on the achievable bandwidth and allowed maximum gain [1]–[6]. Because the dynamics of car-like mobile robot (CLMR) possesses nonlinear and coupled features, a networked-based control of CLMR becomes a challenging problem.

Because the decentralized control scheme is free from the difficulties arising from the complexity in design, debugging, data gathering, and storage requirements, it is more preferable to CLMR than centralized control [7], [8]. As one knows, the fuzzy control algorithm [9]–[13] consists of a set of heuristic decision rules and is regarded as a nonmathematical control algorithm. Such a nonmathematical control algorithm has been proven to be very attractive whenever the controlled systems cannot be well defined or modeled. However, it needs a trial-and-error to obtain an acceptable tracking performance. It is well-known that sliding-mode control (SMC) uses discontinuous control action to drive state trajectories toward a specific hyperplane in the state space, and to maintain the state trajectories sliding on the specific hyperplane until the origin of the state space is reached [14], [15]. This principle provides a guidance to design a fuzzy controller for achieving system stability and satisfactory performance. Therefore, the combination of the two control principles is called fuzzy sliding-mode control (FSMC) provides a robust controller for the nonlinear systems [16], [17]. There are *five* control parameters for the FSMC. Two coefficients are first set to obtain the suitable dynamics of the sliding surface, which is the linear combination of present and past tracking error. Based on the practical ranges of the sliding surface and its derivative, two normalizing scaling factors are selected. Finally, the fifth parameter is the output scaling factor, which is chosen according to the system stability.

In the beginning, two FDSMCs with two suitable set of scaling factors for an unloaded CLMR (i.e., the wheels of CLMR do not contact the ground to proceed the control of two motors) is constructed. One is for the steering angle, the other is for the forward–backward velocity. Then, these scaling factors and the coefficients of the sliding surface are applied for the trajectory tracking of the CLMR so that a robust performance is acceptable. The proposed control can track a reference trajectory without the requirement of a mathematical model. Only the information about the upper bound of the CLMR and the delay feature of Internet network and wireless module are needed to choose appropriate scaling factors and coefficients of the sliding surface. To ensure the quality-of-service (QoS), the sampling time of the overall control system must be greater than total transmission time of the closed-loop system (see, e.g., [5] and [6]). Under these circumstances, the stability of the closed-loop system in the face of small time-varying delay is also addressed to satisfy the requirement of the networked-based control.

Finally, a sequence of experiments with different sampling times including: 1) a microprocessor-based FDSMC of CLMR; 2) a PC wireless module-based FDSMC of CLMR; and 3) an Internet network and wireless module-based FDSMC (or

Manuscript received September 1, 2004; revised August 21, 2006. Abstract published on the Internet November 30, 2006. This work was supported in part by the National Council of Science of Taiwan under Grant NSC-93-2218-E-036-003.

C.-L. Hwang is with the Department of Electrical Engineering, Tamkang University, Taipei 25137, Taiwan, R.O.C. (e-mail: chih-lyang_hwang@hotmail.com; clhwang@mail.tku.edu.tw).

L.-J. Chang is with the Department of Mechanical Engineering, Tatung University, Taipei 10451, Taiwan, R.O.C. (e-mail: chang_lijui@hotmail.com).

Y.-S. Yu is with the Toes Opto-Mechatronics Company, Taipei 104, Taiwan, R.O.C.

Color versions of one or more of the figures in this paper are available online at http://ieeexplore.ieee.org.

Digital Object Identifier 10.1109/TIE.2006.888806

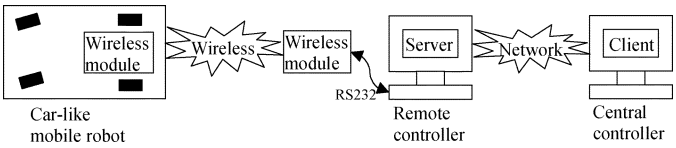

Fig. 1. The experimental setup of NBFDSMC for CLMR.

NBFDSMC) of CLMR, is carried out to confirm the usefulness of the proposed control scheme.

II. System Description and Problem Formulation

A. System Description

Fig. 1 shows the experimental setup of network-based fuzzy decentralized sliding-mode control (NBFDSMC) for a CLMR. The proposed network-based control system includes the following three parts (e.g., [5], [6]): 1) the remote system (i.e., CLMR) and remote controller (i.e., server computer); 2) the central controller (i.e., client computer); and 3) the data network. The central controller possesses high computing power and memory and is not suitable to be installed at the remote site. In this paper, the central controller contains FDSMC and adaptation to the QoS provided by the network. The remote controller is assumed to have enough computing power to do relative simple preprogram, e.g., to calculate the proposed control input, to convert the control signal received from the central controller via internet network into a wireless signal to drive the two motors of the CLMR. In addition, the remote controller can send the local measurements, such as steering angle and forward–backward velocity of the CLMR, back to the central controller through the Internet network. In this paper, the client and server computers use transmission control protocol (TCP) as the layer-4 protocol on the Internet protocol (IP) network.

The main feature of network-based control is time-delay occurred in the data network or wireless module. Define the time delay in transmitting a signal from the client computer to the server computer, and from the server computer to the client computer as $\tau_{\rm cs}$ and $\tau_{\rm sc}$, respectively. Besides, the time-delays occurred in the wireless transmitting from the server computer to the CLMR and from the CLMR to the server computer is defined as τ_{sr} and τ_{rs}, respectively. Because the time-delays of the proposed controller and the CLMR are smaller than the delay in the data network or wireless transmitting, these delays are ignored. One factor of interest in this paper is the selection of the sampling time h for the proposed control system. The following criterion: $h > \tau_t \geq \tau_{\rm cs} + \tau_{\rm sc} + \tau_{sr} + \tau_{rs}$ is used to ensure the QoS of the Internet network and wireless module. Together with a smaller gain for a larger sampling time, the scaling factors and coefficient of the sliding surface for FDSMC are adjusted to obtain a satisfactory performance [5], [6].

The CLMR with two wheels driving system is depicted in Fig. 2. The rear wheels are fixed parallel to the car chassis; the single front wheel can turn to the right or left. The kinematic constraint of a nonholonomic mobile robot is described as follows (cf. [18]–[22]):

$$-\dot{x}(t)\sin\sigma(t) + \dot{y}(t)\cos\sigma(t) = 0. \tag{1}$$

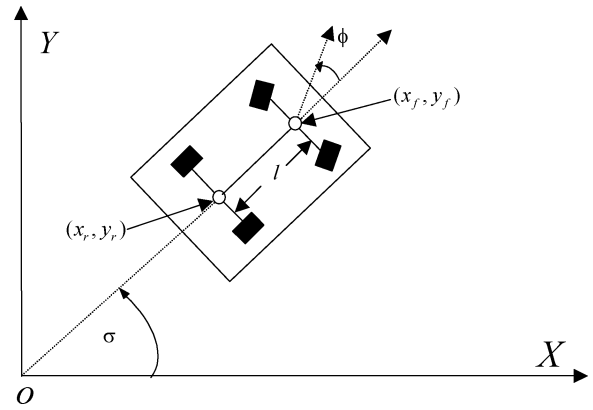

Fig. 2. Kinematic model of a CLMR.

The velocity parameters of the CLMR are expressed as follows:

$$\dot{x}_r(t) = v\cos(\sigma), \dot{y}_r(t) = v\sin(\sigma), \text{ and } \dot{\sigma}(t) = \frac{v\tan(\phi)}{l} \tag{2}$$

where (x_r, y_r) denotes the position of the rear-wheel center of the CLMR, $\sigma(t)$ is the angle between the orientation of the CLMR and the X-direction, ϕ is the orientation of the steering wheel with respect to the frame of the CLMR (i.e., steering angle), ν denotes the speed of the longitude (i.e., forward–backward velocity), and l is the wheelbase of the CLMR. Similarly, the kinematics model of the front-wheel of the CLMR is given as follows:

$$\dot{x}_f(t) = v\cos(\sigma), \dot{y}_f(t) = v\sin(\sigma), \text{ and } \dot{\sigma}(t) = \frac{v\tan(\phi)}{l}. \tag{3}$$

Equation (2) of (3) is applied to calculate a planning trajectory. A real trajectory of the CLMR is detected by a CCD camera (see Fig. 4).

The realization of a CLMR is depicted in Fig. 3 including two servo DC motors with one pulsewidth modulation (PWM) driver, one microprocessor, one wireless module, and some mechanisms. Front wheel and rear wheel are individually driven by the same permanent magnet DC motor. Table I shows the basic specifications of the CLMR. The corresponding specifications of the DC motor and PWM driver are described as follows.

1) Motor (A-max 32 motor from the Maxon Company): graphite brushes, 20 W, no load speed 6420 rpm, maximum continuous torque 0.0473 Nm, maximum continuous current 1.35 A, torque constant 0.0351 Nm/A, mechanical time constant 0.014 s, rotor inertia 43 $\mathrm{g.cm^2}$, length 61.5 mm, and mass 242 g.
2) Gear box (GP-32C from Maxon): gear ratio 51:1 (front wheel) and 36:1 (rear wheel), maximum permissible radial load (12 mm from flange) 140 N, maximum continuous torque at gear output 6 Nm, maximum efficiency 70%, mass inertia 0.7 $\mathrm{g.cm^2}$, length 43 mm, and weight 194 g.
3) Digital encoder: $2+1$ index channel, 500 counts per turn, maximum operating frequency 100 kHz, length 18.3 mm, and weight 90 g.

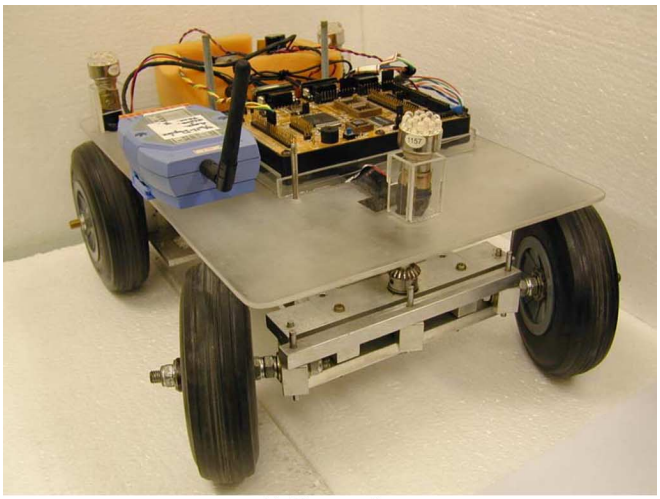

(a) Photograph.

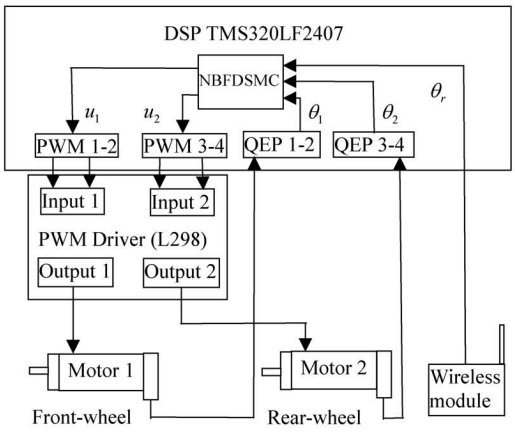

(b) Block diagram.

Fig. 3. Realization of the CLMR.

4) Driver (L298): an integrated monolithic circuit in a 15-lead multiwatt, and PowerSO20 package, high voltage (up to 46 volt), high current (up to 4 A), and dual full-bridge driver.

The core of the CLMR is the digital signal processing (DSP) of TMS320LF2407. Its hardware includes general purpose (GP) timers, analog/digital converter (ADC), full-compare/PWM units, capture units, quadrature-enecoders pulse (QEP), series port (e.g., series communication interface (SCI), series peripheral interface (SPI), control array network (CAN), and interface of joint test action group (JTAG).

The SST-2450 is a spread-spectrum radio modem controlling an RS-232/RS-485 interface port. It is used for data acquisition and transmission between the server computer and the CLMR. Its operating frequency range is between 2410.496 and 2471.936 MHz.

The image system to detect the response of trajectory is introduced as follows. The interpolation method to obtain world coordinate (OXY) from image coordinate $(O_iX_iY_i)$ is used in this paper. This is a real-world plane grabbed by CCD with the coordinate $(O_cX_cY_c)$; the point (320,480) pixel on the image plane is defined as (0, 0) *cm* on the world coordinate. Because a CCD is not faced squarely to a plane in the world coordinate, an image of a plane in the world coordinate becomes a trapezium (the length of upper side and lower side is 2250 and 1450 mm,

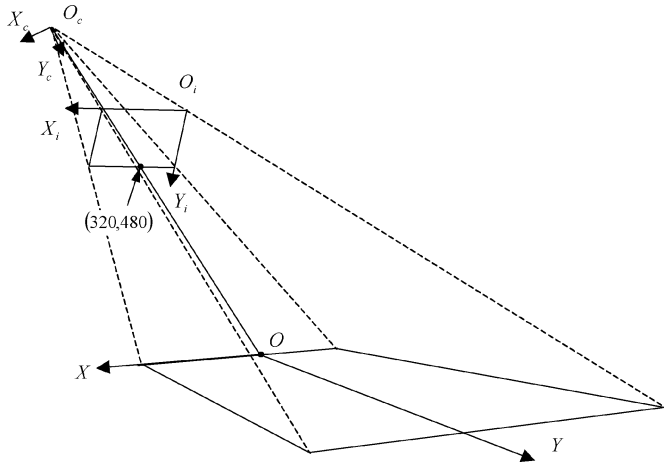

Fig. 4. Definition of various coordinates.

TABLE I
BASIC SPECIFICATIONS OF THE CLMR

Car-Like Mobile Robot	Length	38.7*cm*
	Width	29.5*cm*
	Height	15*cm*
	Weight	5.5 *kg*
Front- and Rear-Wheel	Diameter	12.7*cm*
	Thickness	4*cm*
	Wheelbase	25.5*cm*

respectively, and the depth is 3300 mm). Due to the distortion of the image plane, a straight line on the image plane is shown as an oblique line in the world coordinate. Similarly, a straight line in the world coordinate becomes an oblique line on the image plane (see Fig. 4).

B. Problem Formulation

The above section has described various hardware of the experimental setup. The software in this paper contains: 1) the code composer for editing and downloading the control program to DSP; 2) the FDSMC algorithm in DSP written by C language; and 3) various programs for (a) the transmission of a reference trajectory from PC to DSP; (b) the generation of a PWM signal; (c) image processing; and (d) the decode of the position of the motor. Then, two DC servo motors for the front wheel and real wheel of the CLMR are controlled by the individual FSMC. It is so-called FDSMC. Although two DC motors are successfully controlled by FDSMC, the weight of CLMR is much larger than that of the DC motor and the dynamics of the CLMR is different from that of the DC motor. In this situation, the dynamics of two DC motors is subjected to unmodeled dynamics. Fortunately, the FDSMC possesses strong robustness to cope with this situation. The comparisons between the FDSMC and proportional-integral-derivative (PID) control are also given in Figs. 7–14.

Due to the transmission of control input and system output via the Internet network and the wireless module, the delay feature of the signal occurs. Based on the previous studies [1]–[6], the feedback control in the face of time-delay always results in a limit on the achievable bandwidth and allowed maximum gain. Under these circumstances, the scaling factor and the coefficients of the sliding surface should be revised according to

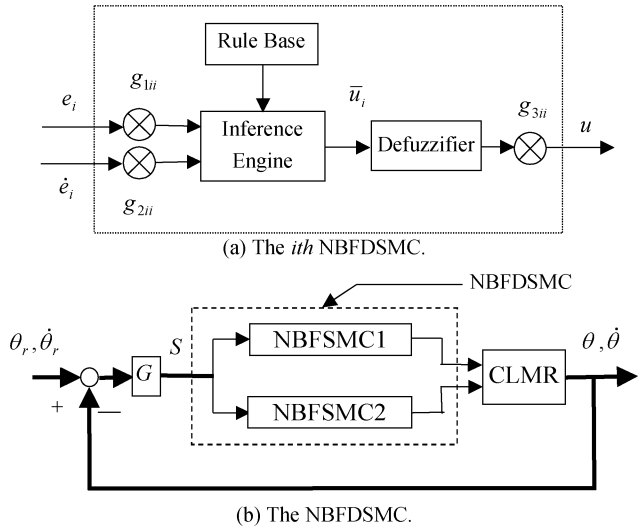

Fig. 5. Block diagram of NBFDSMC .

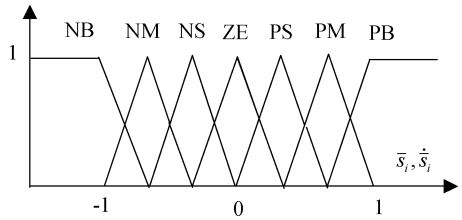

Fig. 6. Membership function with triangular type.

different conditions so that the system response can be compensated without the risk of instability.

Finally, the main subject of this study is to investigate a network-based control of CLMR. As one knows, an Internet network possesses a random time-delay; the instability of the closed-loop system through an Internet network often occurs. Because the wireless module also possesses a delay characteristic, the NBFDSMC for a CLMR becomes a challenging problem. The stability of the closed-loop system with the subjection of small time-varying delay is also investigated. Under some suitable conditions, the uniformly ultimately bounded tracking result can be assured. Three categories of experiments are implemented in this paper: 1) a microprocessor-based FDSMC of CLMR,; 2) a PC wireless module-based FDSMC of CLMR; and 3) an Internet network and wireless module-based FDSMC (or NBFDSMC) of CLMR. Moreover, different sampling times for the closed-loop system are adopted to ensure the QoS. Together with a smaller gain for a larger sampling time, a sequence of experiments is employed to examine their corresponding responses.

III. Fuzzy Decentralized Sliding-Mode Control (FDSMC)

Consider the following CLMR (see, e.g., [23]):

$$A(\theta)\ddot{\theta}(t) + B(\theta, \dot{\theta}) + C(\theta) + N(t) = DU(t) \qquad (4)$$

where $\theta(t) \in \Re^2$ is the angle of the CLMR, $A(\theta) \in \Re^{2\times 2}$ denotes the inertia matrix of positive definite for any

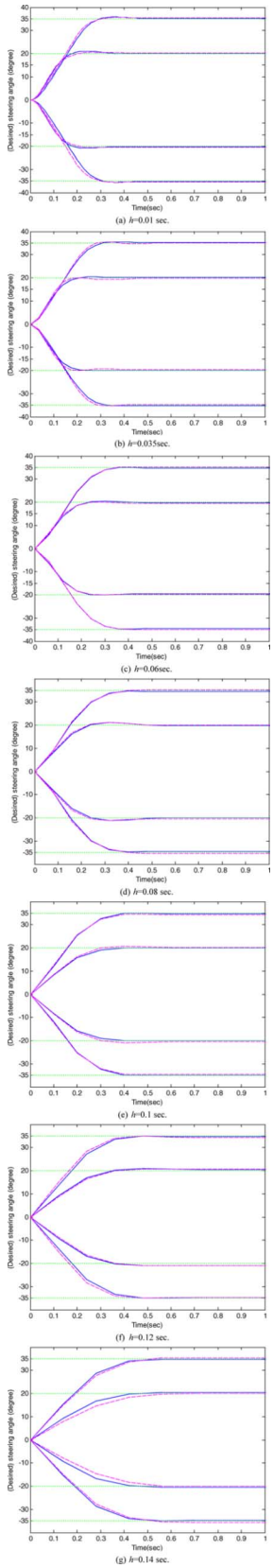

Fig. 7. The responses of NBFDSMC $(-)$ and PID control $(---)$ of front wheel for different desired steering angles $(\cdots)$ and different h.

$\theta(t), B(\theta, \dot{\theta}) \in \Re^2$ comprises the centrifugal, Coriolis torques, $C(\theta) \in \Re^2$ denotes the gravitational torque, $N(t)$ denotes a nonlinear time-varying uncertainty, $D \in \Re^{2\times 2}$ represents the

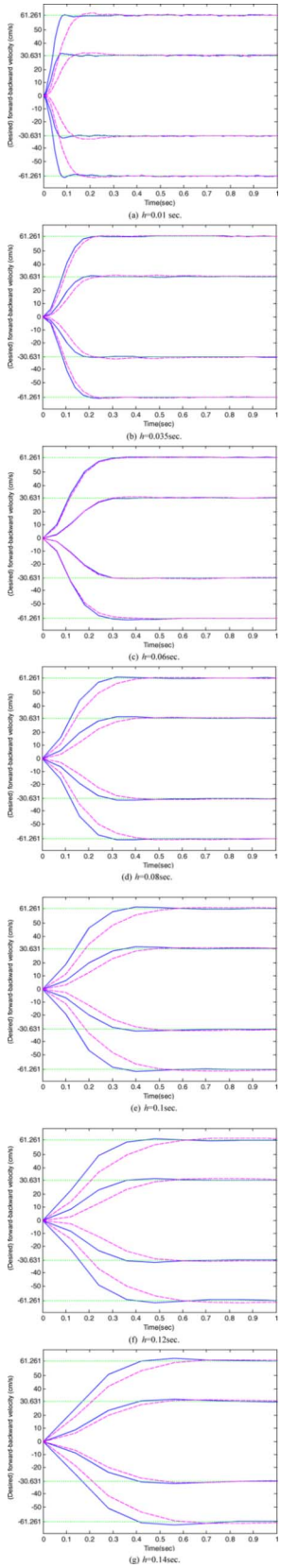

Fig. 8. The responses of NBFDSMC $(-)$ and PID control $(---)$ of rear wheel for different desired forward–backward velocities $(\cdots)$ and different h.

control gain, and $U(t) \in \Re^2$ is the control torque. It is assumed that the dynamics of (4) is unknown. However, the upper bound of function from (4) is supposed to be known.

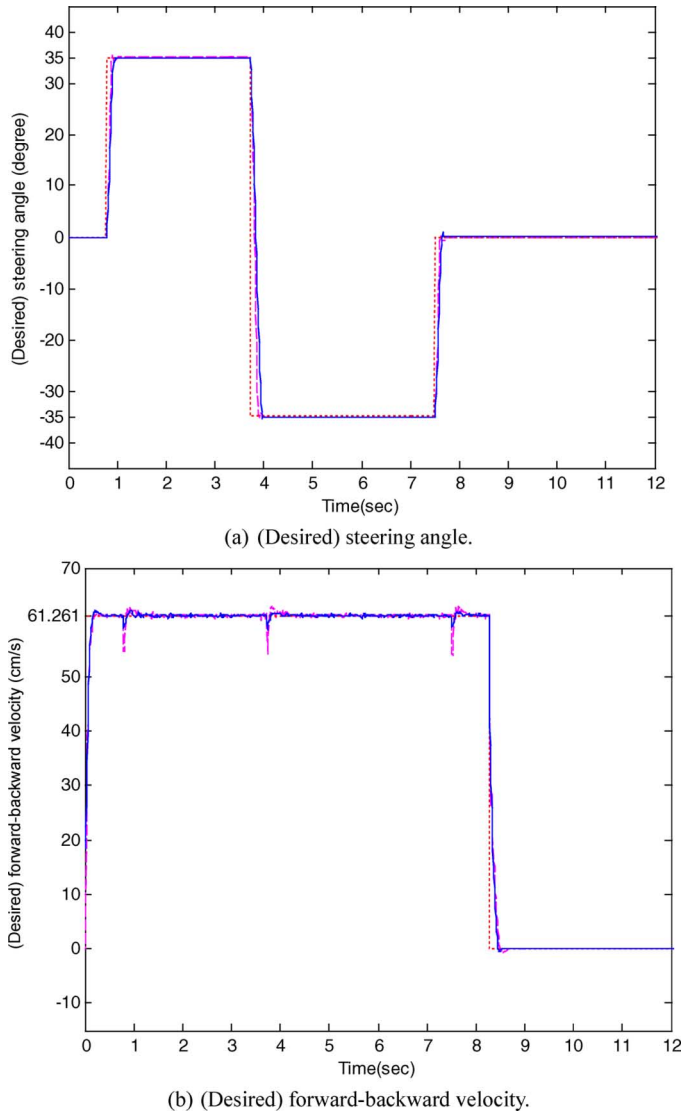

Fig. 9. The responses of trajectory tracking of case 1 for desired steering angle $(\cdots)$ and desired forward–backward velocity $(\cdots)$ in the unloaded condition using NBFDSMC $(-)$ and PID control $(---)$.

The NBFDSMC includes two parallel NBFSMCs (cf. Fig. 5), and it has two sliding surfaces shown as follows:

$$S(t) = GE(t),\ G = [\,G_1 \quad G_2\,],\ E(t) = [\,E_1^T(t) \quad E_2^T(t)\,]^T \tag{5}$$

where $S(t) \in \Re^2$, $G_1 = \mathrm{diag}(g_{1ii}) > 0$, $G_2 = \mathrm{diag}(g_{2ii}) > 0 \in \Re^{2\times 2}$, $i = 1, 2$ are the coefficients of sliding surface, and

$$E_1(t) = \theta_r(t) - \theta(t),\ E_2(t) = \dot{E}_1(t) \tag{6}$$

where $\theta_r(t) \in \Re^2$ is a reference trajectory, $E_1(t) = [e_1(t)e_2(t)]^T$, and $E_2(t) = [e_3(t)e_4(t)]^T$. From (4) and (6), it leads to

$$\dot{E}_2(t) = \ddot{\theta}_r(t) - A^{-1}(\theta)\left\{DU(t) - B(\theta,\dot{\theta}) - C(\theta) - N(t)\right\}. \tag{7}$$

The output of the NBFDSMC is designed as follows:

$$\begin{aligned} U(t) &= G_3\overline{U}(t) = G_3\left[GE_\tau(t) + \Delta\mathrm{sgn}(GE_\tau)\right] \\ &= G_3\left[S_\tau(t) + \Delta\mathrm{sgn}(S_\tau)\right] \end{aligned} \tag{8}$$

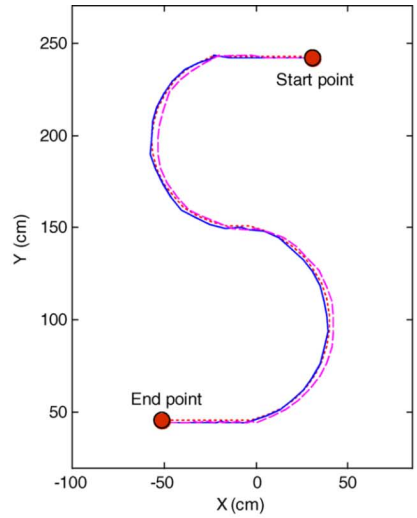

(a) Planning and real trajectory.

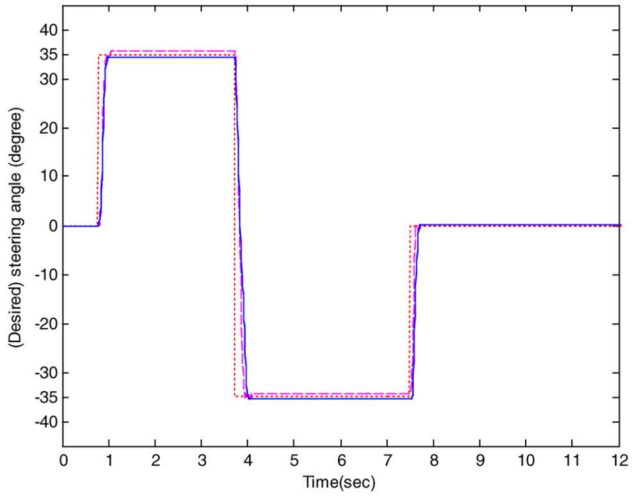

(b) (Desired) steering angle.

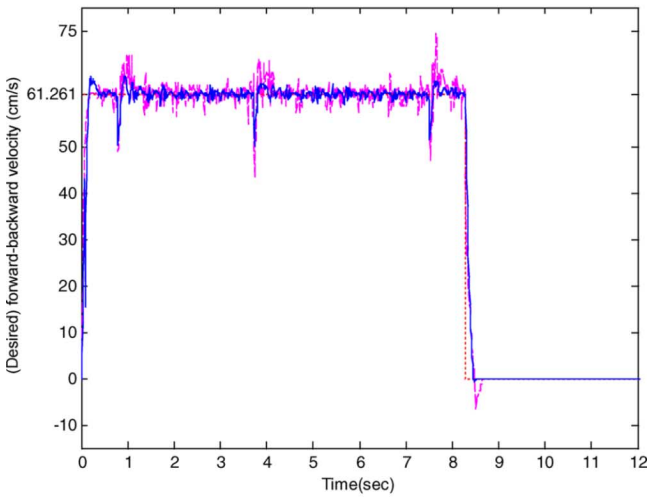

(c) (Desired) forward-backward velocity.

Fig. 10. The responses of trajectory tracking of case 1 for desired steering angle $(\cdots)$ and desired forward–backward velocity $(\cdots)$ using NBFDSMC $(-)$ and PID control $(---)$.

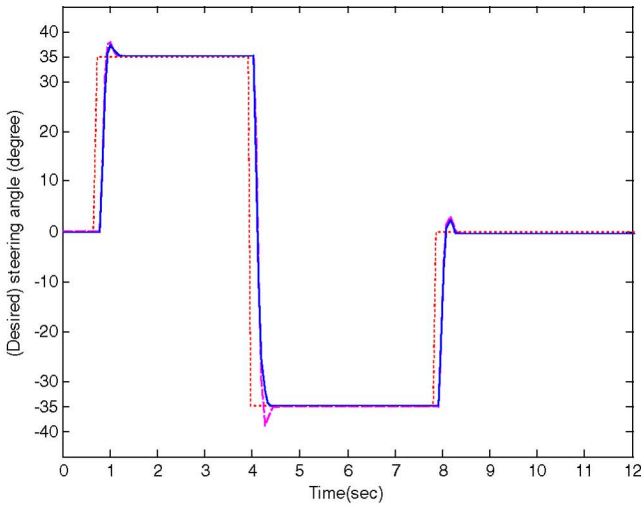

(a) (Desired) steering angle.

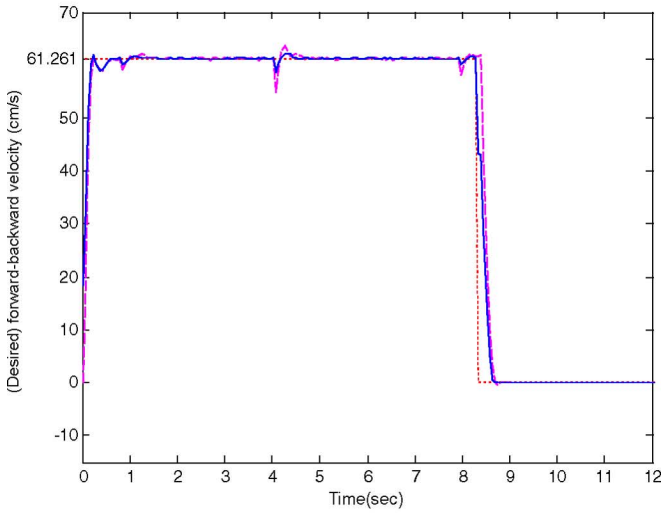

(b) (Desired) forward-backward velocity

Fig. 11. The responses of trajectory tracking of case 2 for desired steering angle $(\cdots)$ and desired forward–backward velocity $(\cdots)$ in the unloaded condition using NBFDSMC $(-)$ and PID control $(---)$.

where $S_\tau(t) = S(t-\tau(t))$, $E_\tau(t) = E(t-\tau(t))$, $\tau(t)$ denotes a time-varying delay with an upper bound τ_u, which is caused by the transmission delay of the signal through the Internet network and wireless module, $G_3 = \text{diag}(g_{3ii}) > 0 \in \Re^{2\times 2}$ is the output scaling factor, $\overline{U}(t)$ is the fuzzy variable of $U(t)$, and $\Delta = \text{diag}(\delta_{ii}) > 0 \in \Re^{2\times 2}$. It is assumed that

$$g_{3ii} \geq \frac{\{a_M d_M [|f_i(t)| + \lambda_i]\}}{(g_{2m}\delta_{ii})} \text{ for } i = 1, 2 \tag{9}$$

where $\lambda_i > 0$, $g_{2m} = \lambda_{\min}\{G_2\}$, $a_M = \lambda_{\max}\{A(\theta)\}$, $d_M = \lambda_{\max}\{D\}$, $f_i(t)$ is the ith element of the following matrix:

$$F(t) = G_1\left[\dot{\theta}_r(t) - \dot{\theta}(t)\right] + G_2\left\{\ddot{\theta}_r(t) + A^{-1}(\theta)\left[B(\theta,\dot{\theta}) + C(\theta) + N(t) - DG_3S_\tau(t)\right]\right\}. \tag{10}$$

Before discussing the NBFDSMC in *Theorem 1*, the following definition about uniformly ultimately bounded (UUB)

and the result of a bounded-input-bounded-output for a linear stable system are described.

Definition 1 [24]: The solutions of a dynamic system are said to be UUB if there exist positive constants υ and κ, and for every $\delta \in (0, \kappa)$ there is a positive constant $T = T(\delta)$, such that $\|x(t_0)\| < \delta \Rightarrow \|x(t)\| \leq \upsilon, \forall t \geq t_0 + T$.

Lemma 1 [25]: Consider a linear stable system $\dot{e}(t) + c_1 e(t) = s(t)$, where $c_1 > 0$ and $|s(t)| \leq \alpha \forall t$. Then, $|e(t)| \leq \alpha/c_1$ and $|\dot{e}(t)| \leq 2\alpha$ as $t \to \infty$.

Theorem 1: Applying the NBFDSMC (8) to the unknown system (4) with the satisfaction of condition (9) gives that $\{S(t), U(t)\}$ are UUB and a finite time [see (17)] reaches a convex set of the sliding surface

$$\Omega = \{ S(t) | \|S(t)\| \leq c_s(\tau_u), \text{ with the possibility } \operatorname{sgn}(S) \neq \operatorname{sgn}(S_\tau)\} \quad (11)$$

where $c_s(\tau_u)$ is a positive constant dependent on the upper bound of time-varying delay $\|S(t_0)\| > c_s(\tau_u)$, and t_0 denotes an initial time. If $\tau(t) = 0$, i.e., $c_s(\tau_u) = 0$, then $E(t) \to 0$ as $t \to \infty$.

Proof: Define the following Lyapunov function:

$$V(t) = \frac{S^T(t)S(t)}{2} > 0, \text{ as } S(t) \neq 0. \quad (12)$$

Taking the time derivative of (12) gives

$$\dot{V}(t) = S^T(t)\dot{S}(t). \quad (13)$$

Substituting (6) and (7) into (13) gives

$$\dot{V}(t) = S^T(t)\Big\{ G_1 \left[\dot{\theta}_r(t) - \dot{\theta}(t)\right] + G_2 \left[\ddot{\theta}_r(t) + A^{-1}(\theta)\left(B(\theta,\dot{\theta}) + C(\theta) + N(t) - DU(t)\right)\right]\Big\}. \quad (14)$$

Substituting (8) and (10) into (14) yields

$$\begin{aligned}\dot{V}(t) =& S^T(t)\Big\{ G_1 \left[\dot{\theta}_r(t) - \dot{\theta}(t)\right] \\ &+ G_2 \left[\ddot{\theta}_r(t) + A^{-1}(\theta)\left(B(\theta,\dot{\theta}) + C(\theta) + N(t)\right)\right]\Big\} \\ &- S^T(t)G_2A^{-1}(\theta)DG_3\left[S_\tau(t) + \Delta \operatorname{sgn}(S_\tau)\right] \\ =& S^T(t)F(t) - S^T(t)G_2A^{-1}(\theta)DG_3\Delta \operatorname{sgn}(S) \\ &- S^T(t)G_2A^{-1}(\theta)DG_3\Delta\left[\operatorname{sgn}(S_\tau) - \operatorname{sgn}(S)\right]. \end{aligned} \quad (15)$$

If the sliding surface is outside of the convex set Ω, i.e., $\|S(t)\| > c_s(\tau_u)$, then $\operatorname{sgn}(S) = \operatorname{sgn}(S_\tau)$. Substituting this fact into (15) and using the result $G_2A^{-1}(\theta)D > 0$, yields

$$\begin{aligned}\dot{V}(t) &\leq \|S(t)\| \sum_{i=1}^{2} \left\{ |f_i(t)| - \frac{g_{2m}g_{3ii}\delta_{ii}}{(a_M d_M)} \right\} \\ &= -\|S(t)\| \sum_{i=1}^{2} \lambda_i \leq -\lambda \|S(t)\| = -\lambda\sqrt{2V(t)} \end{aligned} \quad (16)$$

where $\lambda = \min_{1 \leq i \leq 2} (\lambda_i)$. Then, the solution of the inequality (16) for the initial time t_0 and the initial value $S(t_0)$ is expressed as follows:

$$t - t_0 \leq \frac{[\|S(t_0)\| - c_s]}{\lambda} \quad (17)$$

where t denotes the time the operating point hits the boundary of the convex set of the sliding surface (11), and $t - t_0$ denotes the finite time to approach the convex set. Once the operating point reaches the convex set, the tracking error is bounded. From (5) and (8), $\{S(t), U(t)\}$ are then UUB. Based on *Lemma 1*, $|e_i(t)| \leq c_s(\tau_u)/(g_{1ii}/g_{2ii})$ and $|\dot{e}_i(t)| \leq 2c_s(\tau_u)$, $i = 1, 2$ as $t \to \infty$. If $\tau(t) = 0$, then $c_s(\tau_u) = 0$ and the asymptotical tracking is obtained. Q.E.D.

Remark 1: If the operating point is outside of the convex set (11) and the inequality (9) is not satisfied, a larger convex set of sliding surface as compared with (11) can exist such that a finite time reaches this convex set and the sequences $\{S(t), U(t)\}$ are UUB. For simplicity, the detail is omitted.

Remark 2: From (14), it is assumed that $\dot{s}_i(t)$ increases as $u_i(t) = g_{3ii}\overline{u}_i(t)$ decreases, and if $s_i(t) > 0$, then increasing $u_i(t)$ will result in decreasing $s_i(t)\dot{s}_i(t)$ and if $s_i(t) < 0$, then decreasing $u_i(t)$ will result in decreasing $s_i(t)\dot{s}_i(t)$. That is, the control input $u_i(t)$ is designed in an attempt to satisfy the inequality $s_i(t)\dot{s}_i(t) < 0$.

Remark 3: In the beginning, the fuzzy variable is quantized into the following seven qualitative fuzzy variables: 1) positive big (PB); 2) positive medium (PM); 3) positive small (PS); 4) zero (ZE); 5) negative small (NS); 6) negative medium (NM); and 7) negative big (NB). The inputs of fuzzy variable are defined as follows: $\overline{s}_i(t) = g_{sii}s_i(t)$ and $\dot{\overline{s}}_i(t) = g_{\dot{s}ii}\dot{s}_i(t)$, where $G_s = \operatorname{diag}\{g_{s11}, g_{s22}\}$ and $G_{\dot{s}} = \operatorname{diag}\{g_{\dot{s}11}, g_{\dot{s}22}\}$ are applied to normalize the values $\overline{s}_i(t)$ and $\dot{\overline{s}}_i(t)$ into the interval $[-1, 1]$. There are many types of membership functions, some of which are bell shaped, trapezoidal shaped, and triangular shaped, etc. For simplicity, the triangular type in Fig. 6 is used in this application. The linguistic rule of the ith FDSMC is shown in Table II by which the center of gravity method is employed to form a look-up table in Table III that directly relates the inputs $\overline{s}_i(t)$ and $\dot{\overline{s}}_i(t)$ with the output $\overline{u}_i(t)$. In summary, the control actions of the diagonal terms in Table III are ZE. This arrangement is similar to a variable structure controller that has a switching surface. In addition, the control actions of the upper triangle terms are from NS to NB, and those of the lower triangle terms are from PS to PB. It is skew-symmetric.

Based on the system stability (9), the output scaling factor G_3 is chosen. Hence, the real control input $U(t) = G_3\overline{U}(t)$ is obtained to drive the two motors. A larger output scaling factor is set, a smaller tracking error and a faster response are achieved; however, the risk of transient (or unstable) response occurs. Then, a saturation of control input will result in an instability of the closed-loop system. Hence, an appropriate output scaling factor is very important such that the robust performance is accomplished.

IV. Experimental Results

In this section, the experiments are divided into two main parts: 1) the closed-loop response of the unloaded CLMR (i.e.,

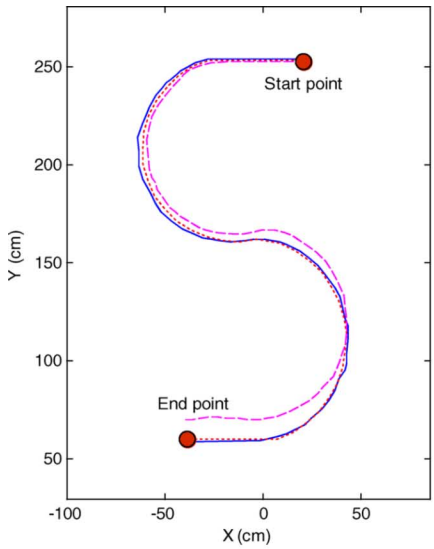

(a) Planning and real trajectory.

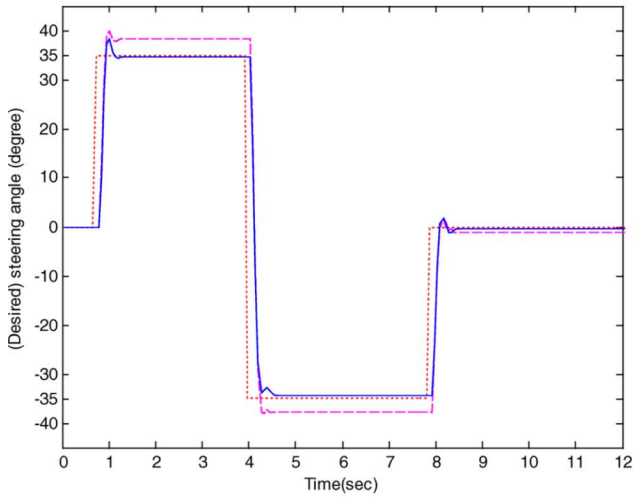

(b) (Desired) steering angle.

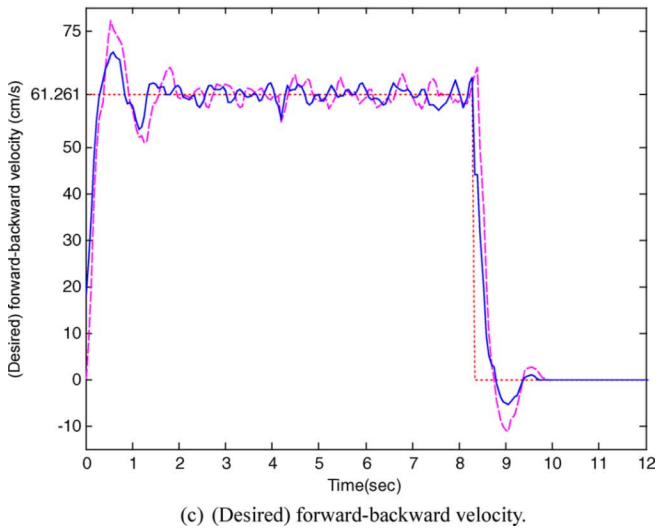

(c) (Desired) forward-backward velocity.

Fig. 12. The responses of trajectory tracking of case 2 for desired steering angle $(\cdots)$ and desired forward–backward velocity $(\cdots)$ using NBFDSMC $(-)$ and PID control $(---)$.

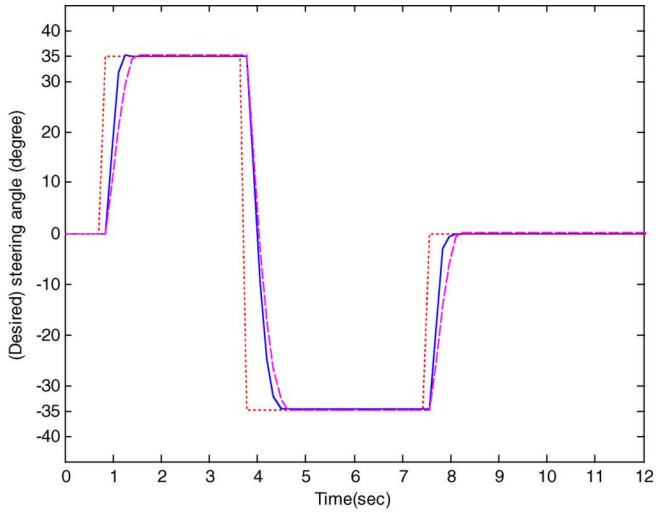

(a) (Desired) steering angle.

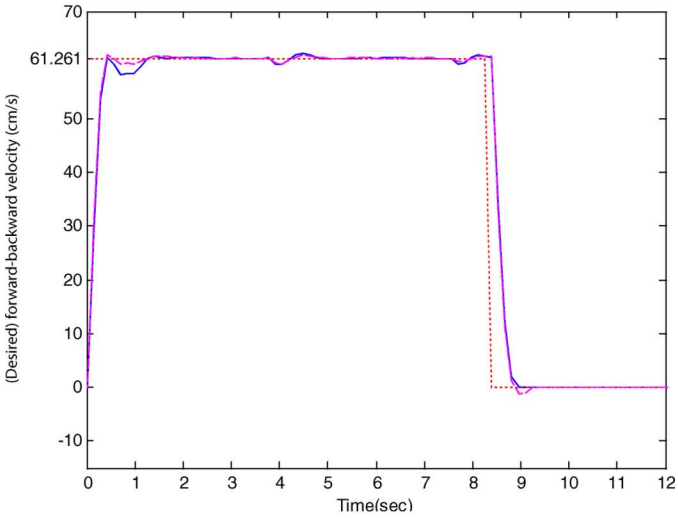

(b) (Desired) forward-backward velocity.

Fig. 13. The responses of trajectory tracking of case 3 for desired steering angle $(\cdots)$ and desired forward–backward velocity $(\cdots)$ in the unloaded condition using NBFDSMC $(-)$ and PID control $(---)$.

the wheels of CLMR do not make contact with the ground to proceed the control of two motors) and 2) the trajectory tracking of curve "S" for the CLMR. The comparisons between the proposed control and PID control are also given to consolidate the usefulness of the proposed method.

A. *Closed-Loop Response of the Unloaded CLMR*

In this subsection, there are three cases: 1) the control input is produced only by the microprocessor on the CLMR without wireless and network transmitting; 2) the control input is calculated by a server computer, and then transmitted to the CLMR by a wireless module; and 3) the control input is calculated in the client computer and transmitted by an Internet network and a wireless module to the CLMR. The discrete form of PID control is described as follows (cf. [26]):

$$u_{PID}(k) = K_p e(k) + \frac{h}{T_i}\sum e(k) + K_p \frac{T_d}{h}\left[e(k) - e(k-1)\right] \tag{18}$$

where K_p, K_i, and K_d denote the gains of proportional, integral, and derivative control, respectively. In this paper, the symbols for the signal to be tracked (or planning trajectory), the response of the proposed control, and the response of PID control

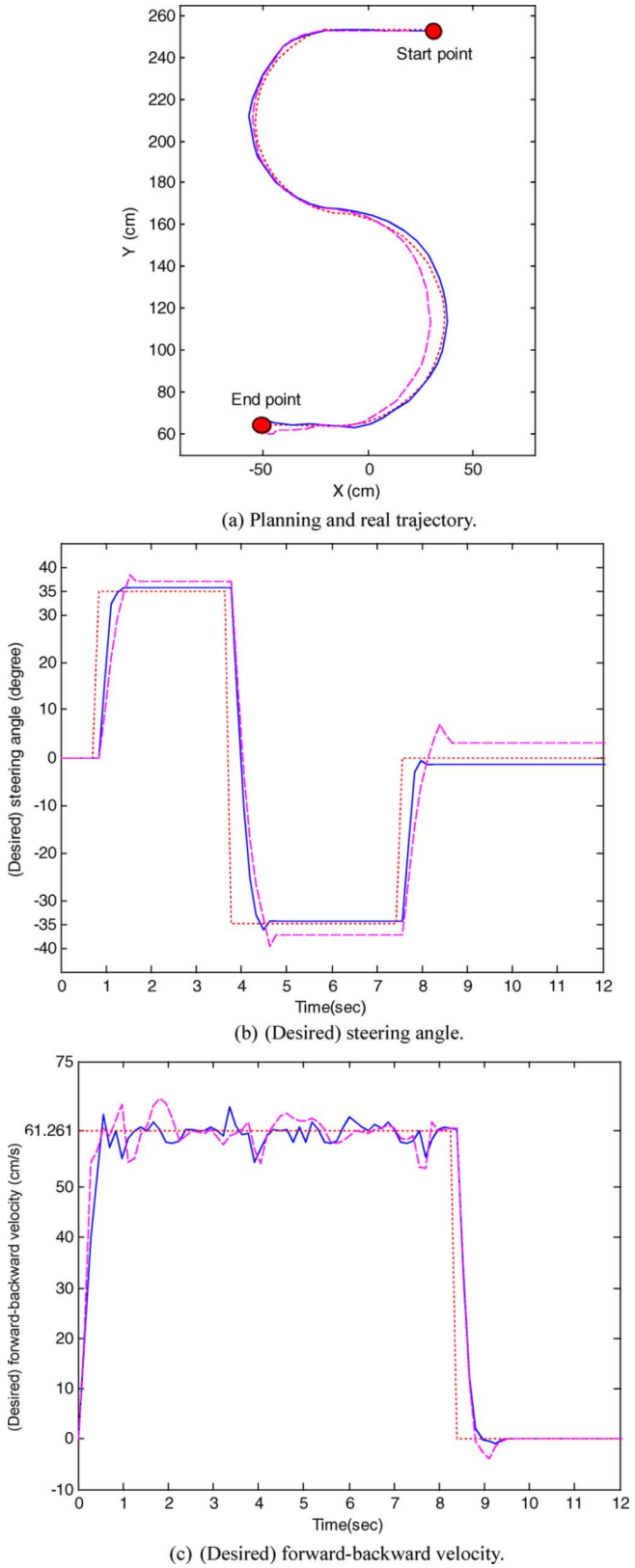

Fig. 14. The responses of trajectory tracking of case 3 for desired steering angle $(\cdots)$ and desired forward–backward velocity $(\cdots)$ using NBFDSMC $(-)$ and PID control $(---)$.

are denoted by the dot line $(\cdots)$, solid line $(-)$, and dash line $(---)$, respectively. Because the subsystem of the steering angle is a type one system, its proposed control input is the

TABLE II
RULE TABLE OF THE iTH FDSMC

$\bar{s}_i$ \ $\dot{\bar{s}}_i$	PB	PM	PS	ZE	NS	NM	NB
NB	ZE	NS	NM	NB	NB	NB	NB
NM	PS	ZE	NS	NM	NB	NB	NB
NS	PM	PS	ZE	NS	NM	NB	NB
ZE	PB	PM	PS	ZE	NS	NM	NB
PS	PB	PB	PM	PS	ZE	NS	NM
PM	PB	PB	PB	PM	PS	ZE	NS
PB	PB	PB	PB	PB	PM	PS	ZE

TABLE III
LOOK-UP TABLE OF THE iTH FSDMC

$\bar{s}_i$ \ $\dot{\bar{s}}_i$	1.0	0.8	0.6	0.4	0.2	0	-0.2	-0.4	-0.6	-0.8	-1.0
-1.0	0.0	-0.2	-0.4	-0.6	-0.7	-0.8	-0.9	-0.95	-1.0	-1.0	-1.0
-0.8	0.2	0.0	-0.2	-0.4	-0.6	-0.7	-0.8	-0.9	-0.95	-1.0	-1.0
-0.6	0.4	0.2	0.0	-0.2	-0.4	-0.6	-0.7	-0.8	-0.9	-0.95	-1.0
-0.4	0.6	0.4	0.2	0.0	-0.2	-0.4	-0.6	-0.7	-0.8	-0.9	-0.95
-0.2	0.7	0.6	0.4	0.2	0.0	-0.2	-0.4	-0.6	-0.7	-0.8	-0.9
0	0.8	0.7	0.6	0.4	0.2	0.0	-0.2	-0.4	-0.6	-0.7	-0.8
0.2	0.9	0.8	0.7	0.6	0.4	0.2	0.0	-0.2	-0.4	-0.6	-0.7
0.4	0.95	0.9	0.8	0.7	0.6	0.4	0.2	0.0	-0.2	-0.4	-0.6
0.6	1.0	0.95	0.9	0.8	0.7	0.6	0.4	0.2	0.0	-0.2	-0.4
0.8	1.0	1.0	0.95	0.9	0.8	0.7	0.6	0.4	0.2	0.0	-0.2
1.0	1.0	1.0	1.0	0.95	0.9	0.8	0.7	0.6	0.4	0.2	0.0

output of the fuzzy table (i.e., Table III) multiplied by an output scaling factor g_{311}, i.e., an absolute control. On the contrary, the second subsystem is the forward–backward velocity control system, i.e., a type zero system. To eliminate the steady-state error, an integrator is used for the output of the fuzzy table (i.e., Table III) multiplied by an output scaling factor, i.e., an incremental control $\Delta u_2(k) = u_2(k) - u_2(k-1)$ (see, e.g., [26]). Alternatively, the second subsystem is thought as a forward–backward velocity control system with an integrator.

To ensure the QoS, different appropriate sampling times for three cases are determined by experiments. In case 1, the sampling period $h = 0.01$ s is selected. In the beginning, the coefficients for the two sliding surfaces are chosen as follows: $g_{111} = 1380$, $g_{211} = 6$, $g_{122} = 109.3$, and $g_{222} = 0.475$. The scaling factors of the FSMC for the front wheel are set as $g_{s11} = g_{211}$, $g_{\dot{s}11} = 50$, and $g_{311} = 10$. The corresponding step responses are shown in Fig. 7(a). The scaling factors of the FSMC for the rear wheel are chosen as $g_{s22} = g_{222}$, $g_{\dot{s}22} = 50$, and $g_{322} = 2$. The relative step responses are presented in Fig. 8(a). Similarly, the scaling factors and the coefficients of the sliding surface for case 1 with $h = 0.005$ s is described in Table IV. For brevity, theses step responses are omitted. In case 2, the sampling period $h = 0.035$ and 0.06 s are chosen. The other selections of the scaling factors (i.e., g_{sii} and $g_{\dot{s}ii}$, $i = 1, 2$) and the coefficients of sliding surface (i.e., g_{1ii} and g_{2ii}, $i = 1, 2$) for the front wheel and rear wheel are also depicted in Table IV; however, g_{311} and g_{322} do not change. The step responses of the front wheel and rear wheel for case 2 are shown in Figs. 7(b) and (c), and 8(b) and (c), respectively. Finally, the sampling period $h = 0.08, 0.1, 0.12,$ and 0.14 s for case 3 are

TABLE IV
SCALING FACTORS AND COEFFICIENTS OF SLIDING SURFACE OF NBFDSMC AND PARAMETERS OF PID CONTROL FOR DIFFERENT SAMPLING TIMES

$h(ms)$	Front-wheel (1st subsystem)								Rear-wheel (2nd subsystem)							
	NBFSMC1				PID control			Fig.	NBFSMC2				PID control			Fig.
	g_{111}	g_{211} $= g_{s11}$	$g_{\dot{s}11}$	g_{311}	K_{p1}	K_{i1}	K_{d1}		g_{122}	g_{222} $= g_{s22}$	$g_{\dot{s}22}$	g_{322}	K_{p2}	K_{i2}	K_{d2}	
5	3220	7	90	10				—	138	0.3	100	2				—
10	1380	6	45	10	20.5	1.8	0.55	7(a)	109.3	0.475	50	2	6.5	85.0	0.06	8(a)
20	518	4.5	22.5	10				—	86.3	0.75	25	2				—
35	233	3.55	12.9	10	9.2	1.3	0.3	7(b)	59.2	0.9	14.3	2	3.5	48.0	0.035	8(b)
40	167	2.9	11.3	10				—	57.5	1	12.5	2				—
50	115	2.5	9	10				—	50.6	1.1	10	2				—
60	96	2.5	7.5	10	4.5	0.8	0.18	7(c)	42.2	1.1	8.3	2	2.5	38.0	0.03	8(c)
70	62	1.9	6.4	10				—	36.1	1.15	7.1	2				—
80	49	1.7	5.6	10	4.2	0.6	0.14	7(d)	33.1	1.15	6.3	2	2.0	24.0	0.03	8(d)
90	40	1.55	5	10				—	30.3	1.15	5.6	2				—
100	33	1.45	4.5	10	3.6	0.4	0.12	7(e)	27.6	1.2	5	2	1.6	16.0	0.03	8(e)
110	28	1.325	4.1	10				—	25.1	1.2	4.5	2				—
120	24	1.25	3.8	10	3.0	0.2	0.09	7(f)	23.0	1.2	4.2	2	1.4	11.5	0.025	8(f)
130	21	1.175	3.5	10				—	21.2	1.2	3.8	2				—
140	18	1.1	3.2	10	2.6	0.2	0.08	7(g)	19.7	1.2	3.6	2	1.2	8.5	0.025	8(g)
150	15	1	3	10				—	18.4	1.2	3.3	2				—

addressed (cf. Table IV). The corresponding step responses of the front wheel and rear wheel are depicted in Figs. 7(d)–(g) and 8(d)–(g), respectively. Similarly, the other scaling factors and the coefficients of the sliding surface of FSMC for different sampling times are also given in Table IV. Their relative step responses are similar with Figs. 7 and 8; for simplicity, those figures are left over. Furthermore, the parameters of PID control for Figs. 7 and 8 are expressed in Table IV.

From (5) and (6), the solution of tracking error is given as follows:

$$e_i(t) = e_i(0)e^{-g_{1ii}t/g_{2ii}} + \int_0^t \frac{e^{-g_{1ii}(t-\tau)/g_{2ii}}s_i(\tau)d\tau}{g_{2ii}}, i = 1, 2. \quad (19)$$

From Table IV, g_{111}/g_{211} is smaller as h is larger; then from (19), the convergent rate of $e_1(t)$ becomes smaller (see Fig. 7). However, $g_{311} = 10$ is large enough to drive the operating point to the sliding surface. In short, the bandwidth of the first subsystem becomes lower as the sampling time is larger. For the second subsystem, g_{122}/g_{222} is also smaller when h is larger; the convergent rate of $e_2(t)$ is smaller, and then the incremental control $\Delta u_2(k)$ becomes smaller as h is larger. It implies that the convergent speed to the sliding surface becomes slower as a larger sampling time is used. Briefly, the larger sampling time is chosen, the system bandwidth becomes smaller. Because the first and second subsystems, respectively, possess an absolute control and an incremental control, $g_{311} = 10 > g_{322} = 2$. In addition, the value of g_{311} and g_{322} should not be too large to prevent a chattering (or transient) response. Then, a possibility of saturated control input results in an instability of the closed-loop system.

As compared with the results of the proposed control and PID control, the responses of the steering angle for the proposed control are only a little better than that of PID control. On the contrary, the responses of the forward–backward velocity control for the proposed control are better than that of PID control. Based on our experimental results, merely using a PID control cannot obtain an acceptable performance, as shown in Figs. 7 and 8. However, an addition of derivative control much improves the system performance. In short, the corresponding experimental results are better than that of previous studies using PID control (e.g., [5] and [6]). More importantly, the fact that the robustness of the proposed control is superior to that of PID control is confirmed by the trajectory tracking of curve "S" in the next subsection.

B. Trajectory Tracking of Curve "S" for the CLMR

Based on the results of Section IV-A, the trajectories tracking three of the above-mentioned cases for the proposed control and PID control are presented in Figs. 9–14. The scaling factors and coefficients of the sliding surface for the proposed control or the parameters of PID control for the unloaded and trajectory tracking of CLMR are the same compare with their robustness. In the experiment, a planning trajectory is obtained from the kinematic model of the CLMR (2). The corresponding real trajectory is achieved by one CCD suspended in a height of 2245 mm (see Fig. 4 for the details). Comparing the results in

Figs. 10(a), 12(a), and 14(a), verifies that the performance and robustness of the proposed control are superior to that of the PID control.

If a complex planning trajectory is assigned, a better tracking result needs a smaller sampling time to obtain an acceptable bandwidth for the proposed control system. In other words, a shorter sampling time for the proposed network-based control system can track a planning trajectory with higher frequency.

V. Conclusion

In this paper, the NBFDSMC for a CLMR is developed. The characteristics of the NBFDSMC for the CLMR are summary as follows.

1) No mathematical model for the little known network-based CLMR is required for the controller design. From the very beginning, the values of G_1 and G_2 are chosen to stabilize the sliding surface with the appropriate dynamics.
2) Only the input–output data pairs are required and the information of the upper bound of system knowledge (e.g., the dynamics of the CLMR, the delay feature of a data network, and wireless module) are needed for the selection of suitable scaling factors.
3) The scaling factors of the proposed control system are adjusted based on the principle: "a larger sampling time using a smaller convergent rate of the operating point" (see Table IV).
4) One interesting factor for the network-based control is the sampling time h. The following criterion $h > \tau_t \geq \tau_{\rm cs} + \tau_{\rm sc} + \tau_{sr} + \tau_{rs}$ is applied to guarantee the QoS.
5) A larger sampling time implies that an achievable bandwidth of the control system is limited (see Figs. 7 and 8).
6) The stability of the closed-loop system in the presence of small time-varying delay is also addressed. There is an upper bound for the stability of the closed-loop system.
7) The robust performance of the proposed control is much better than that of previous studies (e.g., [5] and [6]).

References

[1] R. J. Anderson and M. W. Spong, "Bilateral control of teleoperators with time delay," *IEEE Trans. Automat. Contr.*, vol. 34, pp. 494–501, May 1989.

[2] S. Mascolo, "Smith's principle for congestion control in high-speed data networks," *IEEE Trans. Automat. Contr.*, vol. 45, pp. 358–364, 2000.

[3] S. Munir and W. J. Book, "Internet-based teleoperation using wave variables with prediction," *IEEE/ASME Trans. Mechatron.*, vol. 7, no. 2, pp. 124–133, Feb. 2002.

[4] F. Mazenc, S. Mondi ė, and S. I. Niculescu, "Global asymptotic stabilization for chains of integrators with a delay in the input," *IEEE Trans. Automat. Contr.*, vol. 48, pp. 57–63, Jan. 2003.

[5] M. Y. Chow and Y. Tipsuwan, "Gain adaptation of networked DC motor controllers based on QoS variations," *IEEE Trans. Ind. Electron.*, vol. 50, no. 5, pp. 936–943, Oct. 2003.

[6] Y. Tipsuwan and M. Y. Chow, "Control methodologies in networked control systems," *Contr. Eng. Prac.*, vol. 11, pp. 1099–1111, 2003.

[7] D. D. Sijak, *Large-Scale Dynamic Systems: Stability and Structure*. Amsterdam, The Netherlands: North-Holland, 1978.

[8] E. Freire, T. Bastos-Filho, M. Sarcinelli-Filho, and R. Carelli, "A new mobile robot control approach via fusion of control signal," *IEEE Trans. Syst., Man, Cybern. B*, vol. 34, pp. 419–429, Feb. 2004.

[9] T. J. Procky and E. H. Mamdani, "A linguistic self-organizing process controllers," *IFAC, J. Automatica*, vol. 15, pp. 15–30, 1979.

[10] L. X. Wang and J. M. Mendel, "Generating fuzzy rules by learning from examples," *IEEE Trans. Syst., Man, Cybern. B*, vol. 22, pp. 1414–1427, Nov./Dec. 1992.

[11] Y. S. Kung and C. M. Liaw, "A fuzzy controller improving a linear model following controller for motor drives," *IEEE Trans. Fuzzy Syst.*, vol. 2, pp. 194–202, Aug. 1994.

[12] C. Li and R. Priemer, "Fuzzy control of unknown multiple-input-multiple-output plants," *Fuzzy Sets and Syst.*, vol. 104, pp. 245–267, 1999.

[13] C. L. Hwang and C. Jan, "Optimal and reinforced robustness designs of fuzzy variable structure tracking control for a piezoelectric actuator system," *IEEE Trans. Fuzzy Syst.*, vol. 11, pp. 507–517, Aug. 2003.

[14] Y. Hung, W. Gao, and J. C. Hung, "Variable structure control: A survey," *IEEE Trans. Ind. Electron.*, vol. 40, no. 1, pp. 2–22, Feb. 1993.

[15] C. L. Hwang, "Robust discrete variable structure control with finite-time approach to switching surface," *IFAC, Int. J. Automatica*, vol. 38, no. 1, pp. 167–175, 2002.

[16] G. C. Hwang and S. C. Lin, "A stability approach to fuzzy control design for nonlinear systems," *Fuzzy Sets and Syst.*, vol. 48, pp. 279–287, 1992.

[17] C. L. Hwang and C. W. Hsu, "A thin and deep hole drilling using a fuzzy discrete sliding mode control with a woodpeckering strategy," *Proc. IME J. Syst., Contr. Eng.*, vol. 209, pp. 281–291, 1995.

[18] J. C. Latombe, *Robot Motion Planning*. Norwell, MA: Kluwer, 1991.

[19] L. Podsedkowski, "Path planner for nonholonomic mobile robot with fast replanning procedure," in *Proc. IEEE Int. Conf. Robotics Automation*, Leuven, Belgium, May 1998, pp. 3588–3593.

[20] S. X. Yang and M. Q.-H. Meng, "Real-time collision-free motion planning of a mobile robot using a neural dynamics-based approach," *IEEE Trans. Neural Netw.*, vol. 14, no. 6, pp. 1541–1552, Nov. 2003.

[21] H. Li and S. X. Yang, "Analysis and design of an embedded fuzzy motion controller for a behavior-based nonholonomic mobile robot," in *Proc. IEEE Int. Symp. Intell. Control*, Houston, TX, Oct. 2003, pp. 246–251.

[22] T.-H. S. Li, S. J. Chang, and Y. X. Chen, "Implement of human-like driving skills by autonomous fuzzy behavior control on an FPGA-based car-like mobile robot," *IEEE Trans Ind. Electron.*, vol. 50, no. 5, pp. 867–880, 2003.

[23] R. Fierro and F. L. Lewis, "Control of a nonholonomic mobile robot using neural networks," *IEEE Trans. Neural Netw.*, vol. 9, no. 4, pp. 589–600, May 1998.

[24] H. K. Khalil, *Nonlinear Systems*, 2nd ed. Englewood Cliffs, NJ: Prentice-Hall, 1996.

[25] C. L. Hwang, "Fourier series neural network-based adaptive variable structure control for servo systems with friction," *Proc. IEE -D, Contr. Theory Appl.*, vol. 144, no. 6, pp. 559–565, 1997.

[26] K. J. Aström and B. Wittenmark, *Computer-Controlled Systems—Theory and Design*, 3rd ed. Englewood Cliffs, NJ: Prentice-Hall, 1997.

Chih-Lyang Hwang (A'96) received the B.E. degree in aeronautical engineering from Tamkang University, Taipei, Taiwan, R.O.C., in 1981, and the M.E. and Ph.D. degrees in mechanical engineering from the Tatung Institute of Technology, Taipei, Taiwan, R.O.C., in 1986 and 1990, respectively.

From 1990 to 2006, he had been with the Department of Mechanical Engineering, Tatung Institute of Technology (or Tatung University), where he was engaged in teaching and research in the areas of servo control and control of manufacturing systems and robotic systems. He was a Professor of Mechanical Engineering at the Tatung Institute of Technology (or Tatung University) from 1996–2006. From 1998 to 1999, he was a Research Scholar at the George W. Woodruf School of Mechanical Engineering, Georgia Institute of Technology. Since 2006, he has been a Professor of Electrical Engineering at Tamkang University. At present, he is on the committee of Automation Technology of the National Science Council of Taiwan. He is the author or coauthor of about 100 journal and conference papers. His current research interests include fuzzy (or neural-network) modeling and control, variable structure control, robotics, visual tracking system, and network-based control.

Dr. Hwang received a number of awards, including the Excellent Research Paper Award from the National Science Council of Taiwan and Hsieh-Chih Industry Renaissance Association of Tatung Company. He was a Technical Committee Member of the IEEE IECON'02.

Li-Jui Chang (A'06) was born in Taiwan, R.O.C., in 1983. He received the B.E. and M.E. degrees in mechanical engineering from Tatung University, Taipei, Taiwan, R.O.C., in 2005 and 2006, respectively. He is currently working towards the Ph.D. degree in mechanical engineering at Tatung University.

His current research interests include control system, network-based control, fuzzy control, and mechatronics.

Yuan-Sheng Yu was born in Taiwan, in 1979. He received the M.E. degree in mechanical engineering from Tatung University, Taipei, Taiwan, R.O.C., in 2004.

He is a Professional Engineer at Toes Opto-Mechatronics Company, and an Automation System expert in Taiwan, responsible for automation equipment, robot program, and PLC. His research interests include control system, automation equipment, PLC, and robots.